FOREX Publication
Open Access | Rapid and quality publishing

International Journal of
Electrical and Electronics Research (IJEER)
Research Article | Volume 11, Issue 4 | Pages 1120-1127 | e-ISSN: 2347-470X

The Control of Three-Phase Squirrel Cage Induction Motor by Field Acceleration Method (FAM) for E-Mobility

Elisha Undeti[1*] and Muktevi Chakravarthy[2]
[1]*Research Scholar, Dept. of Electrical Engineering, University College of Engineering, Osmania University, Hyderabad; elisha27u@gmail.com*
[2]*Professor, Dept. of Electrical & Electronics Engineering, Vasavi College of Engineering, Hyderabad; hodeee@staff.vce.ac.in*

***Correspondence:** Mr. U. Elisha, elisha27u@gmail.com

ABSTRACT- The rapid electrification of mobility systems has fuelled the demand for advanced control techniques that can enhance the performance and efficiency of electric vehicles (EVs). In this context, this paper introduces the Field Acceleration Method (FAM) as a control strategy for three-phase squirrel cage induction motors, specifically tailored for e-mobility applications. FAM has not been previously simulated or tested practically in the context of electric mobility, making this study a pioneering effort. Induction motors are widely employed in electric vehicles, and various control methods such as the Indirect Field-Oriented Control (IFOC) gained popularity for its effectiveness in achieving precise and efficient motor control. In this research, FAM is simulated using MATLAB, and the results demonstrate its suitability for electric vehicle control applications. FAM exhibits the potential to achieve rapid speed responses, making it a promising alternative to established control techniques. The outcomes of this study highlight the applicability of FAM in improving the dynamic performance of EVs, contributing to the ongoing efforts to enhance the efficiency and responsiveness of electric mobility solutions. This research paves the way for practical implementations of FAM in electric vehicles, potentially revolutionizing the field of EV motor control.

Keywords: Field Acceleration Method; Induction motor drive; E-mobility; Indirect Field Oriented Control.

ARTICLE INFORMATION
Author(s): Elisha Undeti and Muktevi Chakravarthy;
Received: 26/09/2023; **Accepted**: 25/11/2023; **Published**: 02/12/2023;
e-ISSN: 2347-470X;
Paper Id: IJEER 2609-17;
Citation: 10.37391/IJEER.110432
Webpage-link:
https://ijeer.forexjournal.co.in/archive/volume-11/ijeer-110432.html

Publisher's Note: FOREX Publication stays neutral with regard to Jurisdictional claims in Published maps and institutional affiliations.

1. INTRODUCTION

The growing concern over emissions, global warming, fuel efficiency, and energy resource limitations has led to increased interest in electric and hybrid vehicles among automakers, governments, and consumers. This has created a need for innovative, cost-effective, and efficient hybrid powertrain systems. Modelling and simulation will be crucial for the successful design and development of electric vehicles (EVs), with a particular emphasis on advancing the control technology to meet the evolving demands of this environmentally conscious automotive landscape [1]-[3].

Advancements in power electronics, design tools, and control strategies have led to the maturation of induction motor drives in the context of electric vehicles (EVs). While permanent magnet (PM) brushless motor drives have been widely favored, the induction motor drive is now gaining traction for EVs due to issues like PM material shortages, the high cost of rare-earth PM materials, and the thermal instability of PMs. Its sturdy construction, cost-efficiency, and long-standing technological foundation are anticipated to enable the induction motor drive to retain a significant market presence in EV motor drives in the foreseeable future [4].

Induction motors have a history of being utilized in various types of electric vehicles (EVs), demonstrating respectable performance [4-18]. Notably, they were employed in the General Motors EV1. Furthermore, induction motors are currently used in Tesla EVs, including the Roadster and Model S, Toyota RAV4 [4], Renault Kangoo, Chevrolet Silverado, Daimler Chrysler Durango, Honda Fit EV, REVA NXR, Ford Focus Electric, Ford Transit Connect, as well as BMW X5 [10].

Indirect Field-Oriented Control (IFOC) is a highly popular and widely embraced control method. However, the use of coordinate transformation often introduces unnecessary complexity to the analysis, leading to intricate representations in control circuitry. This complexity can give rise to ambiguous concepts and a higher likelihood of calculation errors when applying vector control theory [19-22].

Field Acceleration Method (FAM), introduced by Yamamura, eliminates the need for a coordinate system, simplifying complexity in control. Consequently, computations become significantly more straightforward. In FAM, direct state variables are employed for induction motor control. The excitation current remains constant and continuous, ensuring a consistent magnitude of the rotating magnetic field. The speed of the field can be altered by adjusting the frequency [23]. FAM's T-1 method is one of the slip control techniques within vector control methods [24]. To further illustrate its

FOREX Publication
Open Access | Rapid and quality publishing
International Journal of Electrical and Electronics Research (IJEER)
Research Article | Volume 11, Issue 4 | Pages 1120-1127 | e-ISSN: 2347-470X

effectiveness, IFOC and FAM are theoretically compared and analyzed, revealing identical results [25,26]. Experimental findings support FAM's efficacy in achieving better speed response characteristics, confirming the validity of the FAM control strategy [27]. In this paper the FAM controlled drive has been proposed for EV application. FAM technique has not been used as a control technique for e-mobility applications. The suitability of FAM controlled drive has been validated by simulation studies. In the next section Field Acceleration Method is presented.

2. FIELD ACCELERATION METHOD (FAM)

2.1 Basics of FAM

Professor Yamamura employed the phase segregation method, wherein a single phase serves as the representative phase. This selection is based on the fact that in the other phases, the solutions remain identical, except for the phase angles, which are sequentially displaced by 2π/3 radians. Circuit equations are formulated separately for one phase on the stator side and one phase on the rotor side. This analytical technique is commonly referred to as the phase segregation method [23].

As per the phase segregation method three phase induction motor equations under steady state are given by.

$$V_1 = R_1 I_1 + j(x_1 + x_m) I_1 + j x_m I_2 \quad (1)$$

$$0 = \frac{R_2}{s} I_2 + j(x_2 + x_m) I_2 + j x_m I_1 \quad (2)$$

In matrix form,

$$\begin{bmatrix} V_1 \\ 0 \end{bmatrix} = \begin{bmatrix} R_1 + jX_1 & jx_m \\ jx_m & \frac{R_2}{s} + jX_2 \end{bmatrix} \begin{bmatrix} I_1 \\ I_2 \end{bmatrix} \quad (3)$$

$$[Z] = \begin{bmatrix} R_1 + jX_1 & jx_m \\ jx_m & \frac{R_2}{s} + jX_2 \end{bmatrix} \quad (4)$$

$[Z]$ is the impedance matrix.

Where $X_1 = (x_1 + x_m)$ (5)

$X_2 = (x_2 + x_m)$ (6)

The secondary currents are transformed by the transformation equation:

$$\begin{bmatrix} I_1 \\ I_2 \end{bmatrix} = \begin{bmatrix} 1 & 0 \\ 0 & \alpha \end{bmatrix} \begin{bmatrix} I_1 \\ I_2^{\alpha} \end{bmatrix} \quad (7)$$

$$C = \begin{bmatrix} 1 & 0 \\ 0 & \alpha \end{bmatrix}$$

Where α is an arbitrary constant

I_2^{α} is the new rotor current,

$$C_t \begin{bmatrix} V_1 \\ 0 \end{bmatrix} = C_t [Z] C \begin{bmatrix} I_1 \\ I_2^{\alpha} \end{bmatrix} \quad (8)$$

From the above we get,

$V_1 = R_1 I_1 + jX_1 I_1 + jx_m \alpha I_2^{\alpha}$ (9)

$0 = \frac{R_2}{s} \alpha^2 I_2^{\alpha} + jX_2 \alpha^2 I_2^{\alpha} + j\alpha x_m I_1$ (10)

$$\begin{bmatrix} V_1 \\ 0 \end{bmatrix} = \begin{bmatrix} R_1 + jX_1 & j\alpha x_m \\ j\alpha x_m & \alpha^2 \frac{R_2}{s} + j\alpha^2 X_2 \end{bmatrix} \begin{bmatrix} I_1 \\ I_2^{\alpha} \end{bmatrix} \quad (11)$$

Corresponding equivalent circuit diagram is drawn based on equation (11) given in *figure 1* and which is called T-type equivalent circuit for steady state operation.

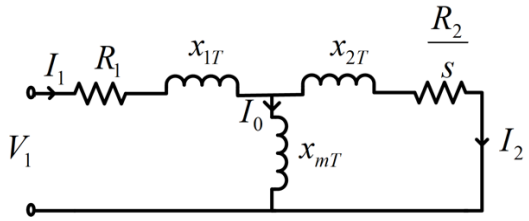

Figure 1: Transformed T type equivalent circuit diagram

Where,

$x_{1T} = X_1 - \alpha x_m$ (12)

$x_{2T} = \alpha^2 X_2 - \alpha x_m$ (13)

$x_{mT} = \alpha x_m$ (14)

$R_{2T} = \alpha^2 R_2$ (15)

From *figure 1*, the primary voltage and primary current remain constant with the transformation mentioned in equation (7). Consequently, the input impedance remains unaffected by the parameter α. However, it's worth noting that the state variables on the secondary side are contingent upon the value of α.

If α is chosen as $\alpha = \frac{x_m}{X_2}$ then the secondary leakage reactance becomes zero

$x_2' = 0$ (16)

$l_2' = 0$ (17)

The equivalent circuit for this value of α, equivalent circuit of *figure 1* is transformed into T-1 type equivalent circuit as depicted in *figure 2*.

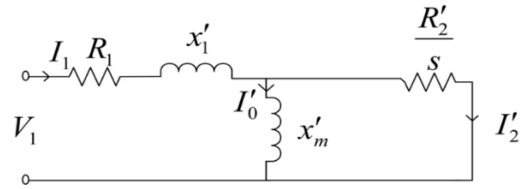

Figure 2: Transformed T-1 type equivalent circuit diagram

Where,

$x_1' = X_1 - \alpha x_m$ (18)

$l_1' = l_1 + L_m - \alpha l_m$ (19)

$x_m' = \alpha x_m$ (20)

$l_m' = \alpha l_m$ (21)

$R_2' = \alpha^2 R_2$ (22)

FOREX Publication
Open Access | Rapid and quality publishing
International Journal of Electrical and Electronics Research (IJEER)
Research Article | Volume 11, Issue 4 | Pages 1120-1127 | e-ISSN: 2347-470X

$$I_2' = \frac{I_2}{\alpha} \quad (23)$$

From T-1 type equivalent circuit diagram in *figure 2*, we can obtain:

The primary current

$$I_1 = I_0' + I_2' \quad (24)$$

$$I_0' = \frac{R_2'/s}{\frac{R_2'}{s}+jx_m'} * I_1 \quad (25)$$

$$I_2' = \frac{jx_m'}{\frac{R_2'}{s}+jx_m'} * I_1 \quad (26)$$

From equation (25),

$$I_1 = \frac{\frac{R_2'}{s}+jx_m'}{\frac{R_2'}{s}} * I_0' \quad (27)$$

$$I_2' = \frac{jsx_m'}{R_2'} * I_0' \quad (28)$$

Torque per phase is given by,

$$T_1 = \frac{P}{2} * \frac{P_g}{\omega} \quad (29)$$

$$P_g = |I_2'|^2 * \frac{R_2'}{s} \quad (30)$$

$$T_1 = \frac{P}{2} * \frac{|I_2'|^2}{\omega} * \frac{R_2'}{s} \quad (31)$$

$$T_1 = \frac{P}{2} * \frac{R_2'}{s\omega} * \left|\frac{sx_m'}{R_2'}\right|^2 * |I_0'|^2 \quad (32)$$

$$T_1 = K_t * sf \text{ at constant } I_0' \quad (33)$$

Where K_t is constant and
sf is the slip frequency.
P is the number of poles.
P_g is the air gap power in watts.
ω is the angular velocity in rad/s.

The relationship between T_1 (torque) and slip frequency, as well as secondary current I_2' (when exciting current I_0' is held constant), is directly proportional. These linear dependencies establish the suitability of T-1 equivalent circuit for the torque control of induction motors. This forms the fundamental basis for FAM control for controlling the speed of induction motor. In FAM, the peak value of the excitation current remains constant and continuous. However, its frequency varies in accordance with the desired motor speed, thereby keeping the magnitude of the rotating magnetic field constant while adjusting its speed in response to the excitation current's frequency. This alteration in frequency directly influences the speed of the rotating magnetic field, consequently affecting the induction motor's speed. By maintaining the excitation current constant, the primary current, secondary current, and torque all become directly proportional to the slip speed, as indicated by *equations (27)*, *(28)*, and *eq. (33)*, respectively. Moreover, the secondary current can be controlled directly by the primary current, as shown in *equation (24)*.

In the next section the electric vehicle power train for FAM controlled induction motor is presented.

2.2 The Electric Vehicle Power Train System

The power train of EV is shown in *figure 3*. The key components of the system include a three-phase induction motor, a battery, FAM controller, and a three-phase voltage source inverter. The driver signals the FAM controller according to speed or torque requirements using the vehicle's accelerator pedal. The FAM controller receives input from both the pedal and the induction motor, including data on motor currents and the actual motor speed. It processes these signals and generates PWM signals, which are given the switching elements through respective gate drives of the voltage source inverter. In the next section FAM controlled drive train is discussed.

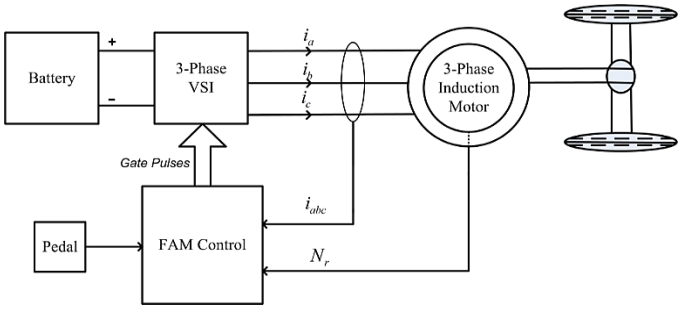

Figure 3: The electric vehicle power train system

2.3 FAM Controlled Drive Train

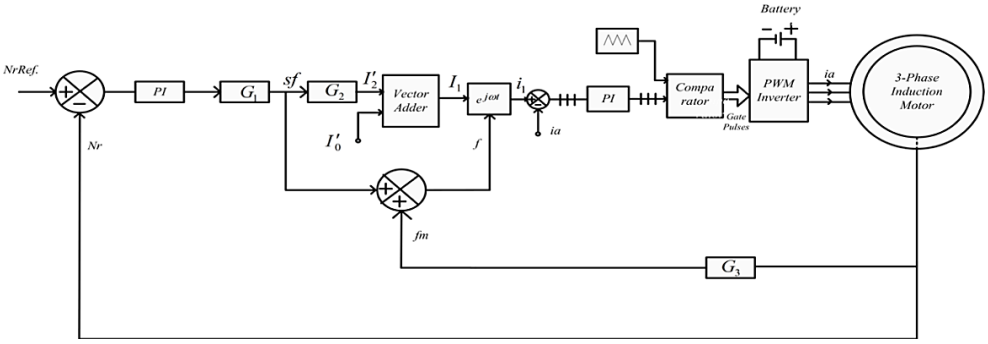

Figure 4: Block diagram of Field Acceleration Method current control of induction motor

FOREX Publication
Open Access | Rapid and quality publishing
International Journal of Electrical and Electronics Research (IJEER)
Research Article | Volume 11, Issue 4 | Pages 1120-1127 | e-ISSN: 2347-470X

Figure 4 presents the block diagram illustrating the Field Acceleration Method (FAM) current control of an induction motor. The control process involves several essential steps: *(a)* Speed controller: The actual speed of the induction motor is compared to the reference speed, resulting in an error signal. This error signal is then processed by a PI controller which multiplies with the motor torque constant to generate a slip frequency (sf) according to the *equation (33). (b)* Primary current calculation: The primary current is determined through vector addition, combining the secondary current and the excitation current, as described in *equation (24). (c)* Primary current frequency computation: The current's frequency is computed by adding the slip frequency to the motor's electrical frequency. *(d)* Instantaneous value of primary current: Using the computed frequency and the peak value of the primary current, the instantaneous value of i_1 (primary current) is obtained. *(e)* Phase currents: Similarly, the other phase currents can be derived by considering a phase difference of $2\pi/3$ radians, as previously mentioned in *section 2.1*.

The phase instantaneous currents are compared with the actual currents of the induction motor and the error signal is processed by PI controller and the output of PI controller are compared with the carrier signal to generate PWM signal. These gate pulses are subsequently applied to the corresponding switches of the voltage source inverter, which is fed from a battery pack.

3. SIMULATION STUDY & RESULTS

The induction motor specifications and parameters are given in the Table 1. The line-to-line voltage of the induction motor is 110V. The output voltage generated by the voltage source inverter is supplied to the three-phase induction motor. It's worth noting that a model-based mathematical models of the voltage source inverter [28] & the induction motor [30] are implemented in MATLAB simulation. The specific ratings and parameters for the induction motor used in this simulation are taken from [6] and motor parameters are given in Table 1. The simulation diagram implemented in MATLAB simulation illustrating the FAM control, Voltage Source Inverter (VSI), and Induction Motor is presented in *figure 5*.

In the context of EVs, electric motors must deliver rapid responses in terms of both speed and torque when starting. Furthermore, when an EV motor experiences sudden load changes, it must swiftly attain a stable state, and speed recovery should be almost instantaneous. Acceleration and deceleration capabilities of electric motors in EVs need to be very fast. Acceleration provides better driving experience, and it is a key selling point for EV manufacturers whereas deceleration is a crucial aspect for vehicle braking system [4-5, 10, 14, 15, 17].

The FAM controlled induction motor is tested under the following conditions in the simulation, and the exciting current remains at a steady peak value of exciting current (Io) consistently during all performance test scenarios. For the EV motor as given in table 1, Io is 4.5793 A. These assessments for the FAM-controlled induction motor encompass various conditions, including motor start-up, reverse operation, lower speeds, abrupt changes in load, as well as acceleration and deceleration tests.

Table 1: Three-Phase Induction Motor Specifications & Parameters

Rated Power	3.73 kW
Rated voltage	110 V
Rated frequency	80 Hz
Number of poles	4
Rated speed	2321 r/min
Rated current	26.73 A
R_s	264.0 mΩ
R_r	423.7 mΩ
L_{ls}	1.4 mH
L_{lr}	1.4 mH
L_m	27.7 mH

The line-to-line voltage of the motor is 110 V. The inverter is fed from a battery pack of 180 V DC. In case of sinusoidal PWM inverter the input DC of the inverter can be calculated by using:

$$V_L = 0.612 * m_a * V_{dc} \quad (34)$$

Where m_a is the modulation index. The above *equation (34)* is described in [29]

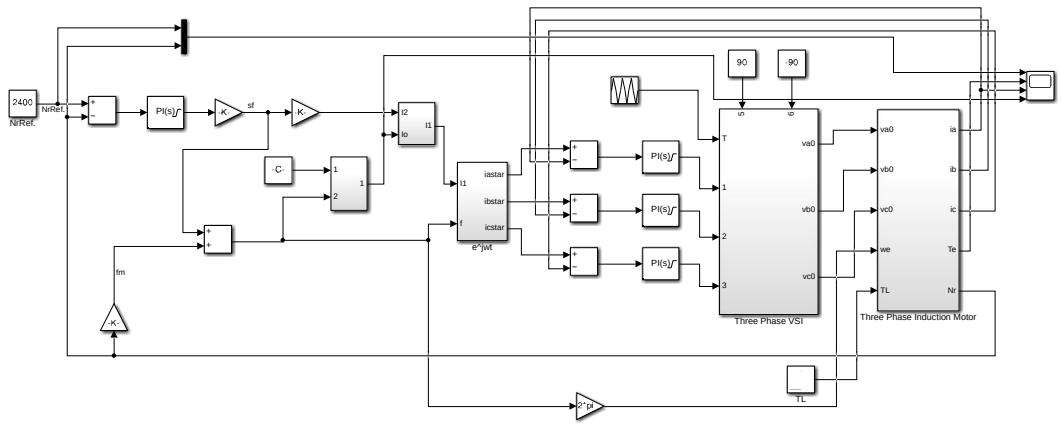

Figure 5: Simulation diagram of Field Acceleration Method current controlled induction motor

FOREX Publication
Open Access | Rapid and quality publishing
International Journal of Electrical and Electronics Research (IJEER)
Research Article | Volume 11, Issue 4 | Pages 1120-1127 | e-ISSN: 2347-470X

Simulation studies have been carried out FAM controlled induction motor drive for various operating conditions and results are described below.

Figure 6 depicts the start-up behaviour of the Field Acceleration Method (FAM)-controlled induction motor. The speed is configured at the rated speed of 2400 r/min. Impressively, the motor attains its specified speed reference within a mere 0.54 seconds. It's noteworthy that the motor speed closely follows the set speed, exhibiting no observable steady-state error during continuous operation. *Figure 7* depicts the reversal of the induction motor's speed. Specifically, at 0.7 seconds, the reference speed transitions from 900 to -900 r/min, and at 1.3 seconds, it reverses from -900 to 900 r/min. In both instances, the torque is consistently maintained at its rated values, and the motor speed accurately tracks the set value. Figure 8. illustrates the motor's behaviour at a lower initial speed reference (ranging from 0 to 300 r/min within one second). In this scenario, the motor speed effectively follows the specified set speed with the slower rate of acceleration.

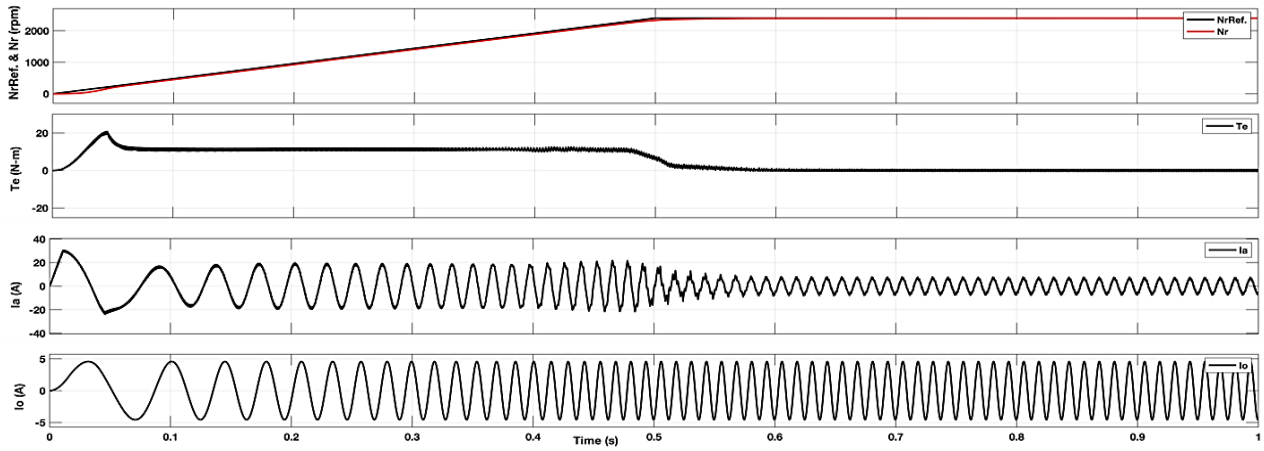

Figure 6: Starting performance of IM drive

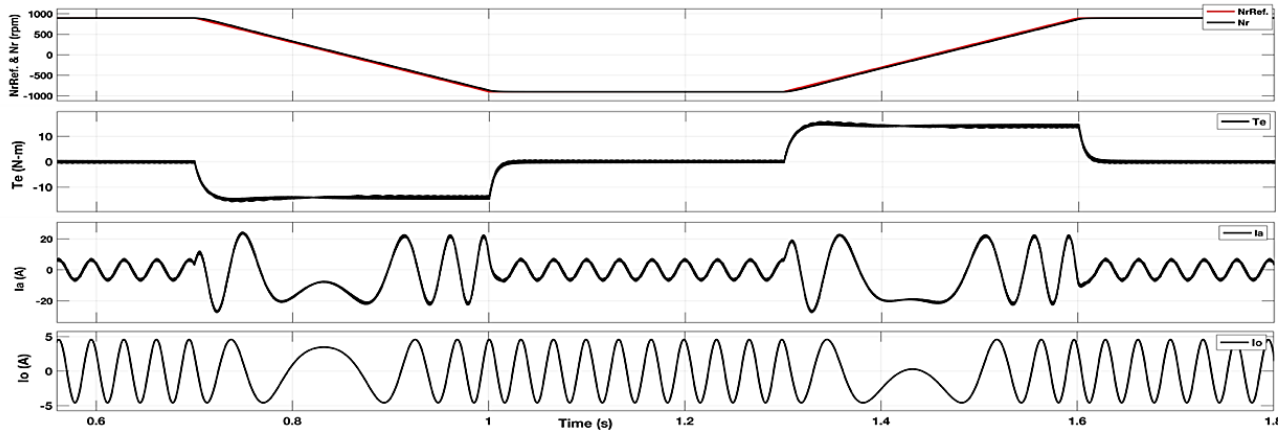

Figure 7: Reverse operation of IM drive

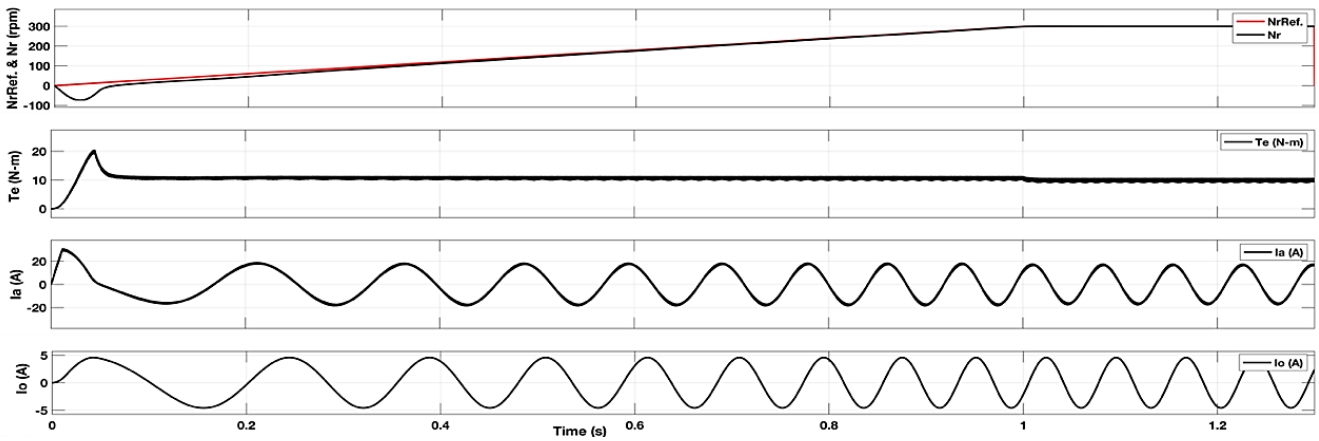

Figure 8: The IM's initial performance with a lower speed reference (300 r/min within one second)

FOREX Publication
Open Access | Rapid and quality publishing
International Journal of Electrical and Electronics Research (IJEER)
Research Article | Volume 11, Issue 4 | Pages 1120-1127 | e-ISSN: 2347-470X

Figure 9 illustrates a situation where the load on the motor is altered, transitioning from 2 to 12 N-m at 0.7 seconds. Impressively, the motor's torque rapidly stabilizes, achieving a steady state within a mere 0.02 seconds. Notably, it's worth mentioning that the Total Harmonic Distortion (THD) in the motor current is measured at 3.74%. Similarly, *figure 10* presents a test involving the sudden removal of load, transitioning from 12 to 2 N-m at 0.7040 seconds. Once again, motor rapidly stabilizes in 0.02 seconds, with a current THD of 8.64%.

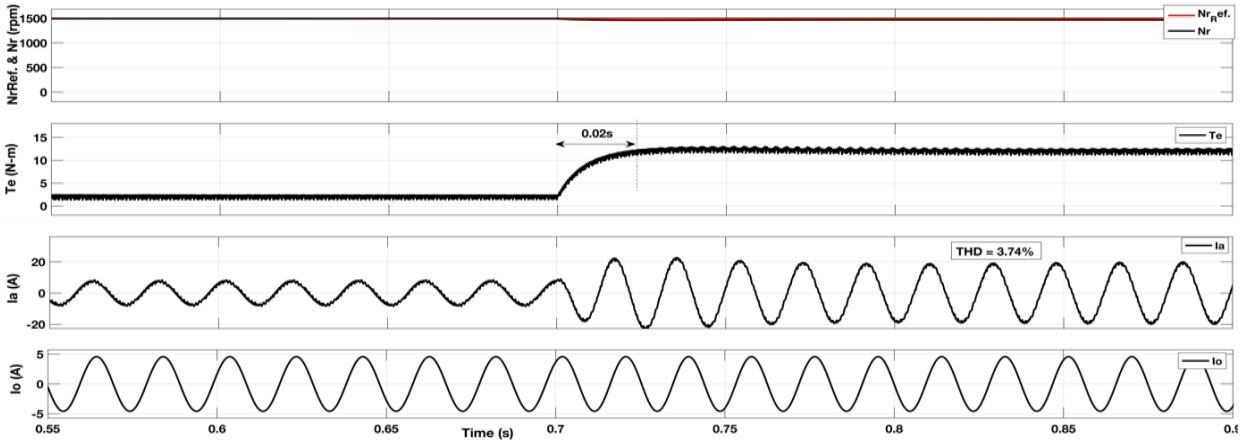

Figure 9: The response of the IM to an abrupt load increase, shifting from 2 to 12 N-m at 0.7s.

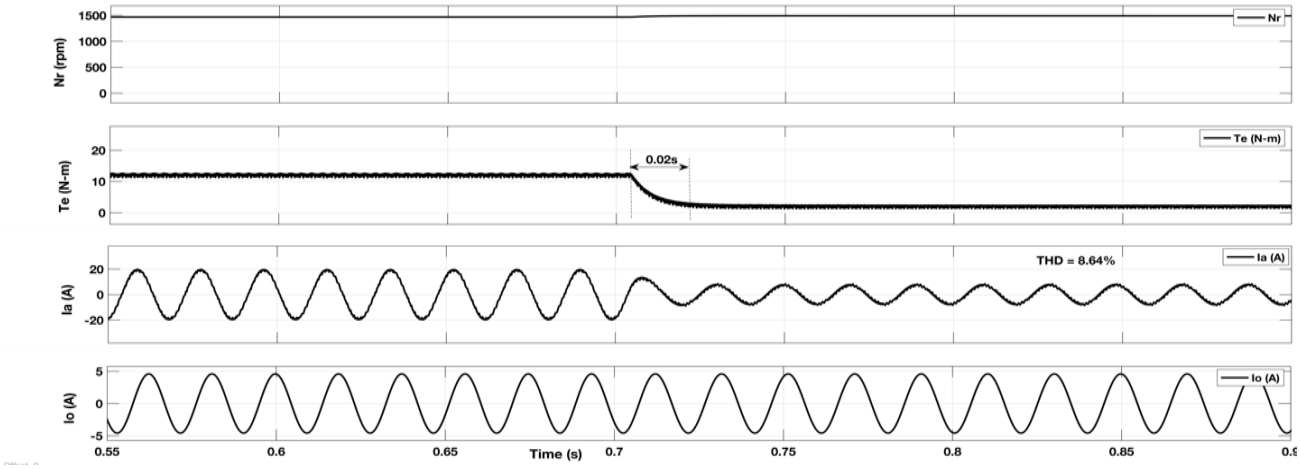

Figure 10: The reaction of the IM to an abrupt load reduction, shifting from 12 to 2 N-m at 0.7040s

Figure 11 illustrates the motor's acceleration as its speed reference transitions from 300 to 2400 r/min at 0.7 seconds. In this scenario, the motor takes 0.4 seconds to attain a steady-state condition. *Figure 12* depicts the deceleration characteristics of the motor as the speed reference transitions from 2400 to 300 r/min at 0.685 seconds, achieving a stable state within 0.3 seconds.

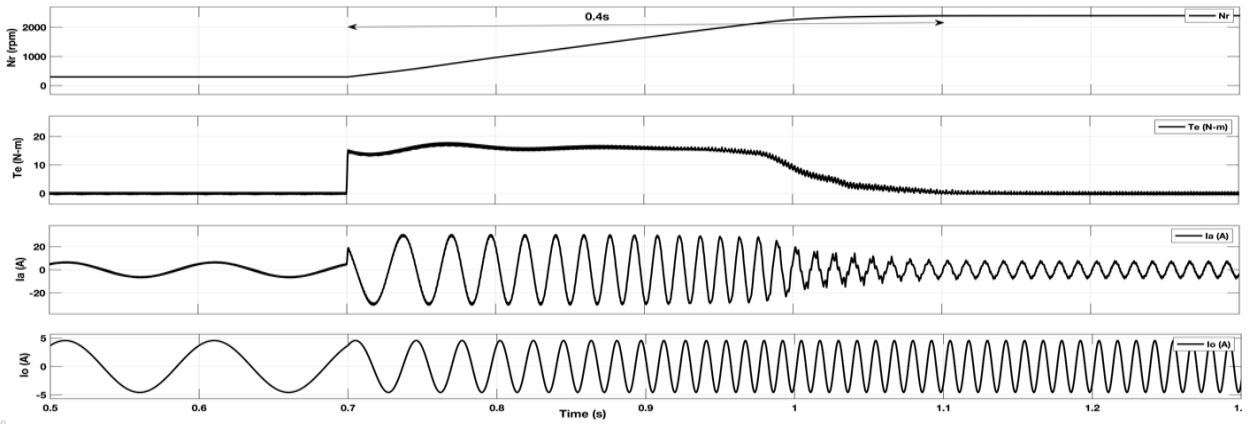

Figure 11: Acceleration performance of IM from 300 r/min to rated rpm at 0.7 sec

FOREX Publication
Open Access | Rapid and quality publishing
International Journal of Electrical and Electronics Research (IJEER)
Research Article | Volume 11, Issue 4 | Pages 1120-1127 | e-ISSN: 2347-470X

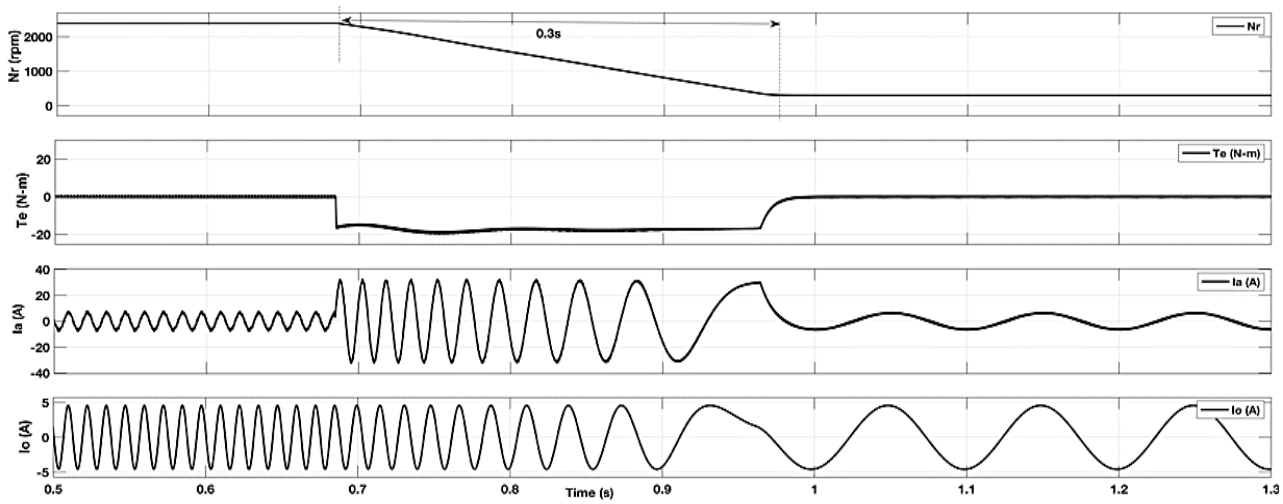

Figure 12: Deceleration performance of IM from rated rpm to 300 r/min at 0.685 sec

4. DISCUSSION

EVs require motor and associated controllers for delivering high starting torque and high dynamic response. In this paper, FAM controlled induction motor drive has been proposed and simulated for EV application.

The simulation studies have been carried out using MATLAB Simulink. The main advantage of FAM lies in its elimination of coordinate transformation systems, unlike traditional field-oriented control methods. FAM's controller is notably straightforward and can be easily implemented without intricate coordination transformations, making it a cost-effective choice compared to other control methods.

In this FAM approach, the exciting current remains constant and continuous, resulting in primary and secondary currents and developed torque that are directly proportional to the slip speed. Consequently, the rotating magnetic field amplitude remains constant, and motor speed is adjusted simply by modifying the frequency.

The FAM-controlled induction motor has been simulated across various operational scenarios, including start-up at rated speed, speed reversal, lower speeds, sudden variations in load torque, and acceleration and deceleration trials. The results indicate that FAM offers rapid response, precise tracking of reference speeds, reduced torque fluctuations, lower Total Harmonic Distortion (THD) in primary current, and exceptionally swift acceleration and deceleration performance.

These findings affirm FAM's suitability for electric vehicle (EV) motor control applications, positioning it as a competitive alternative to existing control methods.

REFERENCES

[1] C. C. Chan, "The state of the art of electric and hybrid vehicles," Proc. IEEE, vol. 90, no. 2, pp. 247–275, Feb. 2002.

[2] A. Emadi, Young Joo Lee, and K. Rajashekara, "Power Electronics and Motor Drives in Electric, Hybrid Electric, and Plug-In Hybrid Electric Vehicles," IEEE Trans. Ind. Electron., vol. 55, no. 6, pp. 2237–2245, Jun. 2008, doi: 10.1109/TIE.2008.922768.

[3] K. Rajashekara, "Present Status and Future Trends in Electric Vehicle Propulsion Technologies," IEEE J. Emerg. Sel. Topics Power Electron., vol. 1, no. 1, pp. 3–10, Mar. 2013, doi: 10.1109/JESTPE.2013.2259614.

[4] K. T. Chau, Electric Vehicle Machines and Drives: Design, Analysis and Application, 1st ed. Chicago, IL, USA: Wiley, 2015.

[5] K. V, R. Rai, and B. Singh, "Sliding Model-Based Predictive Torque Control of Induction Motor for Electric Vehicle," IEEE Trans. on Ind. Applicat., vol. 58, no. 1, pp. 742–752, Jan. 2022, doi: 10.1109/TIA.2021.3131973.

[6] M. J. Akhtar and R. K. Behera, "Space Vector Modulation for Distributed Inverter-Fed Induction Motor Drive for Electric Vehicle Application," IEEE J. Emerg. Sel. Topics Power Electron., vol. 9, no. 1, pp. 379–389, Feb. 2021, doi: 10.1109/JESTPE.2020.2968942.

[7] B. Tabbache, A. Kheloui, and M. E. H. Benbouzid, "Design and control of the induction motor propulsion of an electric vehicle," in Proc. IEEE Veh. Power Propulsion Conf., 2010, pp. 1–6.

[8] Md. J. Akhtar and R. K. Behera, "An analytical design of an induction motor for electric vehicle application," in 2018 IEEE 12th International Conference on Compatibility, Power Electronics and Power Engineering (CPE-POWERENG 2018), Doha: IEEE, Apr. 2018, pp. 1–6. doi: 10.1109/CPE.2018.8372529.

[9] Z. Yang, F. Shang, I. P. Brown, and M. Krishnamurthy, "Comparative Study of Interior Permanent Magnet, Induction, and Switched Reluctance Motor Drives for EV and HEV Applications," IEEE Trans. Transp. Electrific., vol. 1, no. 3, pp. 245–254, Oct. 2015, doi: 10.1109/TTE.2015.2470092.

[10] S. J. Rind, Y. Ren, Y. Hu, J. Wang, and L. Jiang, "Configurations and control of traction motors for electric vehicles: A review," Chin. J. Electr. Eng., vol. 3, no. 3, pp. 1–17, Dec. 2017, doi: 10.23919/CJEE.2017.8250419.

[11] J. Su, R. Gao, and I. Husain, "Model Predictive Control Based Field-Weakening Strategy for Traction EV Used Induction Motor," IEEE Trans. on Ind. Applicat., vol. 54, no. 3, pp. 2295–2305, May 2018, doi: 10.1109/TIA.2017.2787994.

[12] W. Tiecheng, Z. Ping, Z. Qianfan, and C. Shukang, "Design Characteristics of the Induction Motor Used for Hybrid Electric Vehicle," IEEE Trans. on Magn., vol. 4, no. 3, pp. 505-5080, 1/2005.

[13] M. C. Di Piazza, A. Ragusa, and G. Vital, "Effects of common-mode active filtering in induction motor drives for electric vehicles," IEEE Trans. Veh. Technol., vol. 59, no. 6, pp. 2664–2673, Jul. 2010.

[14] M. Farasat, A. M. Trzynadlowski, and M. S. Fadali, "Efficiency improved sensorless control scheme for electric vehicle induction motors," IET Elect. Syst. Transp., vol. 4, no. 4, pp. 122–131, Jul. 2014.

[15] Y. Liu, J. Zhao, R. Wang, and C. Huang, "Performance improvement of induction motor current controllers in field-weakening region for electric

International Journal of Electrical and Electronics Research (IJEER)
Research Article | Volume 11, Issue 4 | Pages 1120-1127 | e-ISSN: 2347-470X

vehicles," IEEE Trans. Power Electron., vol. 28, no. 5, pp. 2468–2482, May 2013.

[16] G. Pellegrino, A. Vagati, B. Boazzo, and P. Guglielmi, "Comparison of induction and PM synchronous motor drives for EV application including design examples," IEEE Trans. Ind. Appl., vol. 48, no. 6, pp. 2322–2332, Nov. 2012.

[17] D. Casadei, M. Mengoni, G. Serra, A. Tani, and L. Zarri, "A control scheme with energy saving and DC-Link overvoltage rejection for induction motor drives of electric vehicles," IEEE Trans. Ind. Appl., vol. 46, no. 4, pp. 1436– 1446, Jul./Aug. 2010.

[18] J. Su, R. Gao, and I. Husain, "Model Predictive Control Based Field-Weakening Strategy for Traction EV Used Induction Motor," IEEE Trans. on Ind. Applicat., vol. 54, no. 3, pp. 2295–2305, May 2018, doi: 10.1109/TIA.2017.2787994.

[19] F. Blaschke, "The principles of field orientation as applied to the new TRANSVEKTOR closed-loop control system for rotating field machines," Siemens Review, pp. 217–220, 1972.

[20] W. Leonhard, Control of Electrical Drives. Berlin, Germany: Springer-Verlag, 1996.

[21] D. Novotny and T. Lipo, Vector Control and Dynamics of AC Drives. Oxford, U.K.: Oxford Univ. Press, 1996.

[22] X. Zhang, "Sensorless induction motor drive using indirect vector controller and sliding-mode observer for electric vehicles," IEEE Trans. Veh. Technol., vol. 62, no. 7, pp. 3010–3018, Sep. 2013.

[23] S. Yamamura, AC Motors for High Performance Applications. New York: Mercel Dekker, 1986.

[24] J. A. Santisteban and R. M. Stephan, "Vector Control Methods for Induction Machines: An Overview," IEEE TRANSACTIONS ON EDUCATION, vol. 44, no. 2, 2001.

[25] Mineo, Eiji Yemada, Katsuhiro Yemada, Jun Oyama, "An Analysis of the Field Acceleration Method and of Vector Control of Induction Motors" Elect. Eng. in Japan, Vol.113, No. 3, 1993.

[26] Richard M Stephan, "Field oriented and field acceleration control for induction motors: Is there a difference?" Proceedings IECON '91: 1991 Int. Conf. on Ind. Electronics, Contr. and Instr., DOI: 10.1109/IECON.1991.239223

[27] Hao Yun, A. K. Behera, Muhammad H. Rashid, "Microcontroller Based Field Acceleration Method Control for Induction Motor with New Digital PWM Inverter Technique", Conf. Record of the 1991 IEEE Industry Applications Society Annual Meeting, DOI: 10.1109/IAS.1991.178084.

[28] B. K. Bose, Modern Power Electronics and AC Drives, Prentice Hall of India, New Delhi, 2001.

[29] Ned Mohan, Tore M. Undeland, William P. Robbins, Power Electronics. Converters, Applications and Design, John Wiley and Sons, Inc, 2003.

[30] B. Ozpineci and L. M. Tolbert, "Simulink implementation of induction machine model - a modular approach," in IEEE International Electric Machines and Drives Conference, 2003. IEMDC'03., Madison, WI, USA: IEEE, 2003, pp. 728–734. doi: 10.1109/IEMDC.2003.1210317.